J Ther Eng, Vol. 9, No. 3, pp. 593−601, May, 2023

Journal of Thermal Engineering
Web page info: https://jten.yildiz.edu.tr
DOI: 10.18186/thermal.1296280

Journal of Thermal Engineering

Research Article

Flow of viscous nanofluids across a non-linear stretching sheet

Pradyumna Kumar PATTNAIK[1], Shoeb Ahmed SYED[2], Sujogya MISHRA[1], Swarnalata JENA[3], Sachindar Kumar ROUT[4,*], Kamalakanta MUDULI[2]

[1]Department of Mathematics, Odisha University of Technology and Research, Bhubaneswar, Odisha 751029, India
[2]Department of Mechanical Engineering, Papua New Guinea University of Technology, Lae, 411, Papua New Guinea
[3]Department of Mathematics, Centurion University of Technology and Management, Odisha, 530013, India
[4]Department of Mechanical Engineering, CV Raman Global University, Bhubaneswar, 752054, India

ARTICLE INFO

Article history
Received: 06 June 2022
Revised: 13 October 2022
Accepted: 15 October 2022

Keywords:
Non-linear Stretching Sheet; Nanofluid; Thermal Radiation; T-Test; Bvp5c

ABSTRACT

This article aims to demonstrate the flow of viscous nanofluid over a non-linear stretching sheet. Considering thermal radiation and dissipative heat in the heat transport phenomenon encourages the flow properties. In generally, nanofluids are employed in heat transfer equipment because they improve the thermal characteristics of coolants present in the equipment. Additionally, these fluids possess unique features that have the potential to be applied in a variety of applications, such as pharmaceutical procedures, hybrid power engines, household refrigerators, grinding, and microchips, among others. Consequently, the current model is built to allow for the optimal selection of thermophysical parameters such as conductivity and viscosity, which will enhance the overall effectiveness of the study. Appropriate transformation rules have been used to modify the highly non-linear PDEs into a couple of highly non-linear ODEs. An efficient built-in MATLAB bvp5C algorithm addresses the boundary value problem under consideration. Using the dimensionless parameters assumed in the problem, changes in the velocity as well as the temperature profiles are shown, and rate coefficients, by using numerical simulations are also employed in tabular form. The important outcomes which are exposed in the study are; that the particle concentration is used as a controlling parameter to reduce the nanofluid velocity, whereas it favours enhancing the fluid temperature and the radiating heat along with the coupling parameter due to the inclusion of dissipative heat also encourages to overshoot the temperature profile.

Cite this article as: Pattnaik PK, Syed SA, Mishra S, Jena S, Rout SK, Muduli K. Flow of viscous nanofluids across a non-linear stretching sheet. J Ther Eng 2023;9(3):593−601.

INTRODUCTION

The mass production, technical, and industrial range of various devices is supported by the research of many scientists and researchers. Timers are used in several industrial devices lower their heat capacity. Researchers have explored a variety of lubricants to see if they may help prevent these issues and keep the temperature inside the device stable. But, the heat storage capacity of these pure liquids is

***Corresponding author.**
*E-mail address: sachindra106@gmail.com

This paper was recommended for publication in revised form by Regional Editor Ahmet Selim Dalkılıç

insufficient for industrial use. The concept of nanofluids has arisen as a result of this. This paper includes a detailed nanofluid model that is intimate. Choi and Eastman [1] sought to test copper water in numerous experimental facilities utilizing pure nanofluids that had improved heat capacity compared to pure liquids, but their experiments were unsuccessful. Rashad et al. [2] examined laminar flow and continuous boundary layer nanofluid flow on a vertical cylinder through a porous medium. As detailed in this work, several associated factors were tested using excellent parametric tests. Ramreddy et al. [3] researched the conductivity of conductive nanofluids flowing over a flat plate. El-Kabeim et al. [4] conducted yet another investigation into the effects of non-administered porous media, heat radiation, and Forchheimer terms on the body. Lin et al. [5] employed Carboxy Methyl Cellulose water with four distinct nanoparticles as the basic solution, then diluted it with water. Mesoporous fluid particles are included in this category, with the deformation of microporous fluid particles being ignored. Many of the flow properties were reproduced in this model. Mishra et al. [6] and Bakar et al. [7] have investigated MHD's natural and forced convection.

The Maxwell model is used to determine which model of the behavior of non-Newtonian fluids is the most accurate. Madhu et al. [8] emphasize the flow of unsteady laminar MHD-Maxwell nanofluids with non-uniform velocities and non-uniform magnetic fields and the flow of unsteady laminar MHD-Maxwell nanofluids with non-uniform magnetic fields. According to Mishra et al. [9], the analysis of viscoelastic fluids' mass and heat transfer was carried out while considering chemical processes and external heating. This problem, known as the von Kalman problem, is employed for infinitely rotating discs in which conductive nanofluids serve as the disc's structural constituents (see [10]). With the help of a Williamson fluid, Qayyum et al. [11] demonstrate the creation of entropy between two rotating discs. In their research, Afridi and Kasim [12] investigated entropy creation by fine needles moving in the centre of parallel currents. The consequences of thermal radiation parameter and dissipation factors are emphasized in this piece of work. Khan et al. [13] investigated a two-dimensional lateral liquid flow that grows toward the blade when the chemical reaction concentration is kept constant. As a result of the originality of the research, the temperature equation now includes a discussion of the impact of heat radiation on heat generation/absorption. A new flow model for nanomaterials has been developed ([14]). In the given paper, Williamson fluids are used to formulate the problem. A numerical study of the flow of viscous and nano liquids on an expanding surface has been carried out by Jena and her co-researchers [15-17]. Magnetic and radiative effects on the water-alumina nanofluids using numerical simulations have been carried out by Sheikholeslami et al. [18].

The application of thermal radiation is useful in various medical treatments like cancer therapy, radiotherapy, blockage removal from arteries, etc. Further, non-Newtonian nanofluid became popular in various oil industries plastic industries because of the high thermal conductivity of the nanoparticle.

The concept of magnetohydrodynamics (MHD) is introduced, which interacts with conductive fluids and magnetic fields in fluid flow to produce a fluid flow. The heat transfer characteristics of the fluid flow system are improved as a result of this procedure. Numerous theoretical, computational, and analytical research [19-21] have been carried out on different nanofluids (MHD) for distinct parametric effects, with the results being compared. Jena et al. [22] made significant contributions to investigating chemical reaction heat transmission in nanofluids and developing mathematical models of porous matrices. Acharya et al. [23] investigated the impacts of thermal energy on viscous fluids by using analytical calculations to theoretically assess the effects of thermal energy. According to several assessments, nanotechnology presents a platform suitable for ultrahigh coolant crises. Tshivhi and Makinde studied the use of nanofluids as coolants in MHDs in which the nanofluid flows over heated contraction/elongation surfaces [24]. Elsaid [25, 26], in a study combining wet cooling towers and vapor compression air conditioning systems, included his Co_3O_4-based and his Al_2O_3-based $H2O/(CH_2OH)_2$ nanofluids in vehicle engine radiators. indicated that Friction coefficients were estimated and used for MgO and TiO2. to the base H_2O nanofluid. Elsaid et al. [27, 28] conducted an exergy analysis on various perforated rib designs utilised in triple tubes heat transfers that used hybrid nanofluids as well as various single and hybrid nanofluids in chilled water to test the stability of air conditioning systems. To make nanofluids better, some more interesting studies [29-31] have been done, which have been considered in the current situation. Hakeem and his coresearchers [32-35] have made a healthy contribution to the field of MHD nanofluid and hybrid nanofluid flow over a stretching sheet.

Formulation of the problem

This article will consider the 2D steady flow of viscous incompressible nanofluids that pass through a non-linearly stretchable surface. Two equally opposite forces constrain the flow near the collapsing plate. The stretching speed of the sheet is $\tilde{u}_w(x) = cx^n$ c, a constant realized by fixing the origin. At the same time, $\tilde{T}_w(x) = T_\infty + bx^m$ is the temperature, $\tilde{T}_w$ wall temperature, and T_∞, ambient temperature were kept on the wall. The coordinate system's physical model (Figure 1) has been followed. The basic equations, i.e., the equation of mass, the equation of momentum, and the energy equation for nanofluids using the general boundary layer approximation, have been considered. Earlier published work [36] is converted to a nanofluid model:

$$\tilde{u}\,\tilde{u}_x + \tilde{v}\,\tilde{u}_y = \upsilon_{nf}\tilde{u}_{yy}$$

$$\tilde{u}_x + \tilde{v}_y = 0,$$

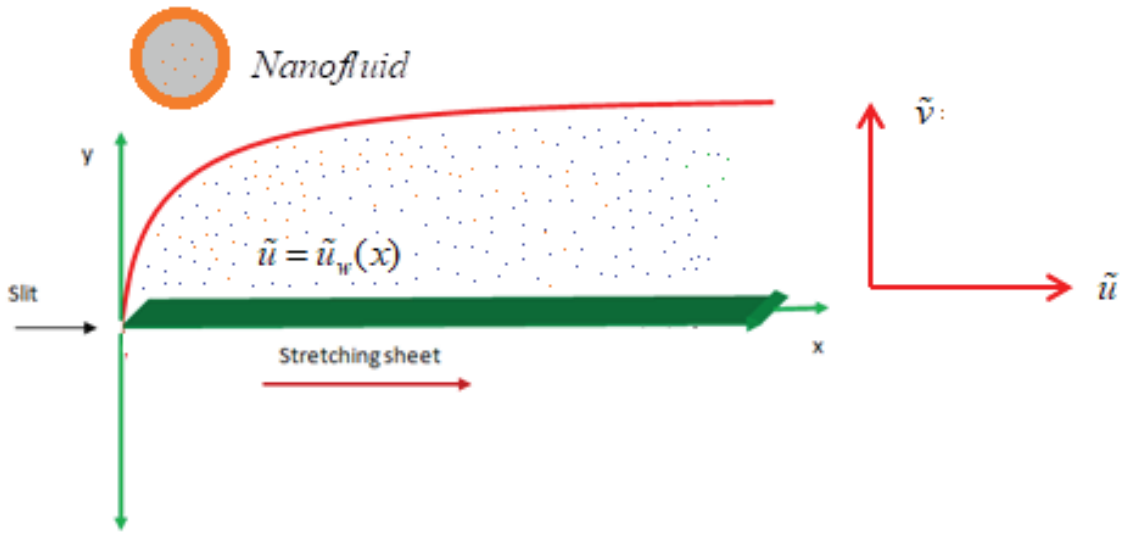

Figure 1. Hemisphere shows the direction of incident radiation and solid angle relations [16].

Equation of Continuity:

$$\tilde{u}_x + \tilde{v}_y = 0, \tag{1}$$

Equation of Momentum:

$$\tilde{u}\,\tilde{u}_x + \tilde{v}\,\tilde{u}_y = \upsilon_{nf}\tilde{u}_{yy} \tag{2}$$

Equation of Energy:

(3)

$$\tilde{u}\tilde{T}_x + \tilde{v}\tilde{T}_y = \frac{k_{nf}}{(\rho c_p)_{nf}}\tilde{T}_{yy} + \frac{\mu_{nf}}{(\rho c_p)_{nf}}\tilde{u}_y^2 - \frac{1}{(\rho c_p)_{nf}}(q_r)_y \tag{4}$$

The converted boundary conditions are:

$$\text{For, } y = 0,\ \tilde{u} = \tilde{u}_w(x), \tilde{v} = 0, \text{ and } \tilde{T} = T_w(x) \tag{5}$$

$$\text{when, } y \to \infty,\ \tilde{u} \to 0 \text{ and } \tilde{T} \to T_\infty \tag{6}$$

The density and effective viscosity (see [17]) of the nanofluid are defined as,

$$\mu_{nf} = \mu_f(1-\phi)^{-2.5}, \frac{k_{nf}}{k_f} = \frac{(\Omega+2)-2\phi(1-\Omega)}{(\Omega+2)+\phi(1-\Omega)}, \Omega = \frac{k_s}{k_f},$$
$$\frac{\rho_{nf}}{\rho_f} = 1-\phi+\frac{\rho_s}{\rho_f}, \frac{(\rho c_p)_{nf}}{(\rho c_p)_f} = 1-\phi+\phi\frac{(\rho c_p)_s}{(\rho c_p)_f}. \tag{7}$$

Radiative heat flux (Rosseland approximation) is ([37]):

$$q_r = -\frac{4\sigma^*}{3k^*}\left[\tilde{T}^4\right]_y \tag{8}$$

Expansion of $\tilde{T}^4$ by the Taylor series method we have (neglecting higher order terms),

$$\tilde{T}^4 \cong 4\tilde{T}T_\infty^3 - 3T_\infty^4$$

Introduction of non-dimensional variables ($m = 2n$):

$$\eta = yx^{\frac{n-1}{2}}\sqrt{\frac{n+1}{\mu_f}}\sqrt{\frac{c}{2}}, \hat{u} = cx^n f', \hat{v} = -\sqrt{c(n+1)}\sqrt{\frac{\mu_f}{2}}\left(f - \eta\frac{n-1}{n+1}f'\right)x^{\frac{n-1}{2}}, \tilde{T} = T_\infty + (T_w - T_\infty)\theta(\eta). \tag{9}$$

causes,

$$\frac{1}{A}f''' - \frac{2n}{n+1}f'^2 + ff'' = 0, \tag{10}$$

$$\frac{1}{\Pr B}\left(\frac{k_{nf}}{k_f} + Nr\right)\theta'' + f\theta' - \frac{4n}{n+1}f'\theta + \frac{A_1}{B}Ecf''^2 = 0 \tag{11}$$

$$\text{for } \eta = 0,\ f = 0,\ f' = 1,\ \text{and } \theta(0) = 1$$

$$\text{when } \eta \to \infty,\ f' \to 0,\ \text{and } \theta \to 0. \tag{12}$$

where,

$$\left.\begin{aligned} A = (1-\phi)^{2.5}\left(1-\phi+\frac{\rho_s}{\rho_f}\phi\right), B = 1-\phi+\frac{(\rho c_p)_s}{(\rho c_p)_f}\phi, \\ \Pr = \frac{\mu_f}{\alpha_f}, Nr = \frac{16k^*}{3\sigma^* T_\infty^3}, Ec = \frac{\tilde{u}_w}{(\rho c_p)_f (T_w - T_\infty)} \end{aligned}\right\} \tag{13}$$

For , Eqns. (9) & (11) gave classical Blasius flat-plate flow problem (see [38]). For (linear stretching), the unique solution of Eqn. (9) can be , whereas there is no exact solution with (non-linearly stretching).

Physical quantities of practical interest

We have studied the skin friction coefficient (C_f) and the local Nusselt number (N_u), which can be defined as:

$$C_f = \frac{\mu_{nf}}{\rho_f}\frac{2}{\tilde{u}_w^2(x)}\left[\tilde{u}_y\right]_{y=0}, Nu = -\frac{k_{nf}}{k_f}\frac{x}{(T_w - T_\infty)}\left[\tilde{T}_y\right]_{y=0}. \tag{14}$$

Putting Eqn. (9) in Eqn. (12), one can get:

$$\sqrt{\frac{c}{2}\frac{x^{n+1}}{\mu_f}}Cf_x = \sqrt{n+1}\frac{f''(0)}{(1-\phi)^{-5/2}}, Nu\sqrt{\frac{\mu_f}{x^{n+1}}}\sqrt{\frac{2}{c}} = -\sqrt{n+1}\left(\frac{k_{nf}}{k_f} + Nr\right)\theta'(0). \tag{15}$$

DISCUSSIONS OF RESULT

The two-dimensional flow of nanofluid over a non-linearly stretching sheet is presented in the current analysis. The role of radiative heat and dissipative heat enriches the flow phenomena. The proposed design model is handled numerically using a suitable built-in MATLAB code bvp5c. Table 1 shows the physical properties of the base fluid (water and Kerosene) and nanoparticle (Copper). Table 2 shows the simulated results of rate coefficients for both the Water and Kerosene-based nanofluids, and these are in good agreement with previous studies of Khan and Pop [39] and Devi and Devi [40]. This can be evident from the numerical calculations of f and Nu .

Further, Table 3 exhibits the numerical results of and for the different restriction values in Water and Kerosene-based nanofluids. In addition, the increase in volume fraction parameter (ϕ), enhances the C_f and N_u. However, the results using Kerosene-based nanofluids dominate over Water-based nanofluids. The non-linear strain parameter (n) reduces but reverses the for both the nanofluids. The Prandtl number increases the Nusselt number, but the radiation parameter and Eckert number have an opposite impact.

Further, a t-test for the skin friction data and the Nusselt number is presented for a confidence level of 95%. The hypothetical test assuming the null mean was rejected for both cases. The results are presented in Table 4. This reveals that the parametric behaviour obtained by the numerically simulated result for the diversified values of the parameters is valid data that will validate the present study. Moreover, a correlation coefficient is calculated with their variances and presented thereat for the paired two-sample mean. Besides that, the computations are obtained numerically and discussed graphically, assuming the assigned values of the parameters , except for the specific variations of the parameter in the corresponding graph.

Figure 2 compares the Cu~Water and Cu~Kerosene nanofluids for the variation of volume fraction (ϕ) on the velocity profile. The flow phenomena are characterized by the thermophysical properties that depend on particle concentration. Therefore the role of particle concentration is vital. It is the amount of dispersion of the solid particles into the base liquid. It is evident that enhanced volume fraction (ϕ) leads to decelerating the velocity distribution because of the heavier density of the solid particles. In a comparative analysis, it is seen that the retardation in the case of Cu~Kerosene is slower than that of Cu~Water because the density of the transported water is slower than that of Kerosene. Figure 3 shows the effect of on the temperature profile considering both the base fluids. When it increases, a slight change will occur. i.e., the profile will increase with increasing . It occurs due to the variation described in an earlier result that particle concentration retards the velocity, and that is the reason the clogging of the particles generates energy near the surface region, and the stored energy gives rise to overshooting the profile, and therefore, the fluid temperature increases significantly. Finally, it is concluded that the magnitude in the case of a Water-based nanofluid is higher than that of a kerosene-based nanofluid. Figures 4 and 5 show the effect of the non-linear stretching parameter (n) on the velocity and temperature profiles. Both profiles decrease with increasing (n) in the nanofluids Copper-Water and Copper-Kerosene. However, due to membrane elongation and wall temperature, the speed and temperature of Copper-Water may be higher than Copper-Kerosene. Figure 6 shows the effect of the Prandtl number on the dimensionless temperature profile considering both the nanofluids. The mathematical description reveals that for the moderate retardation in the thermal diffusivity, the Prandtl number increases, which causes smooth retardation in the fluid temperature, i.e. a purely opposite value lowers the temperature of the fluid and, at the same time, lowers the thermal diffusivity. It is also worth noting that the temperature of Copper-Water is higher than that of Copper-Kerosene. Figures 7 and 8 are drawn for radiation parameters and Eckert numbers, respectively, for the fluid temperature distribution. It is interesting to note that and slowly increases the temperature profile, and in both cases, it was observed that the temperature of the Copper-water was higher than that of the Copper-Kerosene.

Table 1. Thermophysical Properties of Regular and Nanofluids

	c_p (J/KgK)	ρ (Kg/m^3)	κ (W/mK)
Water	4179	997.1	613
Cu	385	8933	400
Kerosene	2090	783	0.145

Table 2. Validation of Nusselt number with Prandtl numbers

Pr	Khan and Pop [39]	Devi and Devi [40]	Present
2	0.9113	0.91135	0.9182732
6.13	----	1.75968	1.7563419
7	1.8954	1.8954	1.8973210
20	3.3539	3.3539	3.3501566

Table 3. Numerical Calculation of Rate Coefficients

ϕ	n	Pr	Nr	Ec	C_f		Nu	
					Water-based	**Kerosene based**	**Water-based**	**Kerosene based**
0.1	0.5	7	0.1	0.5	-1.5155	-1.6154	5.7394	6.1014
0.2					-1.1705	-1.2763	6.6552	7.5322
0					-1.6792	-1.6792	4.9342	4.9342
0.1	1.5				-0.9837	-1.0485	3.5218	3.7438
	2				-1.7217	-1.8353	6.5759	6.9908
	0.5	0.71			-1.5155	-1.6154	1.9226	2.0391
		2			-1.5155	-1.6154	2.9795	3.1661
		7	0.2		-1.5155	-1.6154	6.5708	6.9848
			0.5		-1.5155	-1.6154	6.3329	6.7321
			0.1	0.1	-1.5155	-1.6154	5.7394	6.1014
				0.3	-1.5155	-1.6154	5.5612	5.9112

Table 4. t-Test for Rate Coefficients

	C_f		Nu	
	Water-based	**Kerosene based**	**Water-based**	**Kerosene based**
Mean	-1.46942	-1.55883	5.139355	5.4761
Variance	0.044779	0.045359	2.640415	3.179048
Observations	11	11	11	11
Pearson Correlation	0.988678		0.995563	
Hypothesized Mean Difference	0		0	
df	10		10	
t Stat	9.27407		-4.96054	
P(T<=t) one-tail	1.58E-06		0.000285	
t Critical one-tail	1.812461		1.812461	
P(T<=t) two-tail	3.16E-06		0.00057	
t Critical two-tail	2.228139		2.228139	

Table 5. Validation with previous studies

Authors	Year	Nanofluids	Nanoparticle	Model	Findings
Mohapatra et al. [17]	2019	Water and Kerosene	Copper	Maxwell model	Kerosene is denser in comparison to water, for which the velocity of Cu-water enhances than Cu-kerosene.
Tshivhi et al. [24]	2021	Water	Copper, Aluminium oxide, Iron Oxide	Maxwell model	Cu-water is a better coolant than the other two nanofluids, as this exhibits the highest heat transfer enhancement rate.
Mishra et al. [29]	2022	Water	Copper, Silver	Maxwell model	heat transfer rate rises for the involvement of copper nanoparticles in the dusty fluid, but the reverse result is an encounter for silver.
Pattnaik et al. [30]	2022	Water	Titanium dioxide	Tiwari-Das nanoscale model	The rate of heat transfer is enhanced.

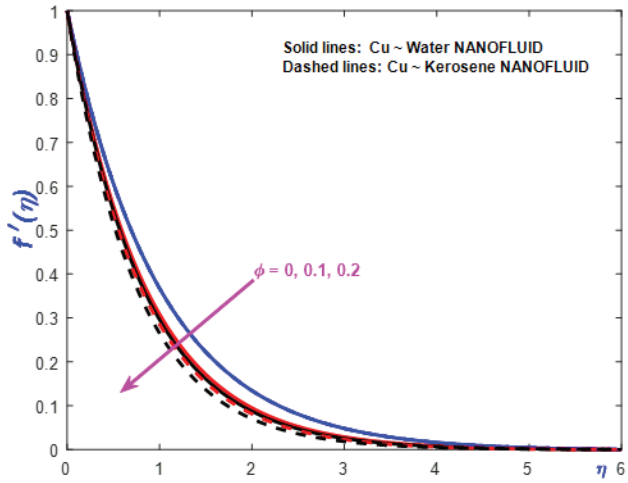

Figure 2. Influence of volume fraction parameter (ϕ) on velocity.

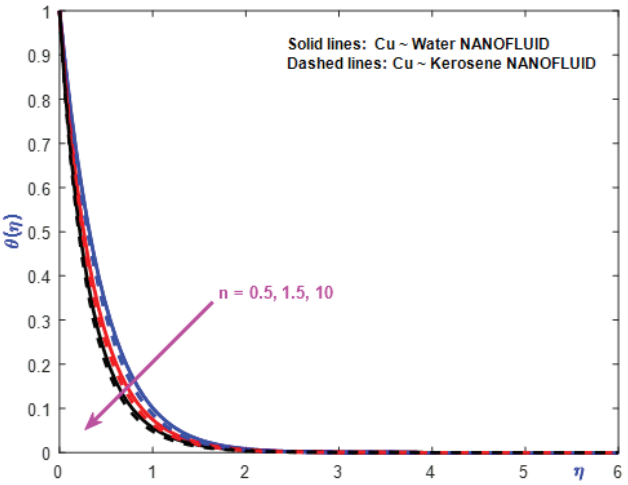

Figure 5. Influence of stretching parameter (n) on temperature.

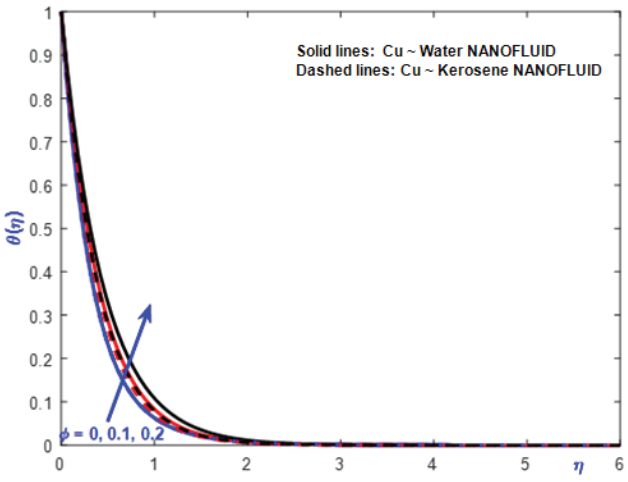

Figure 3. Influence of volume fraction parameter (ϕ) on temperature.

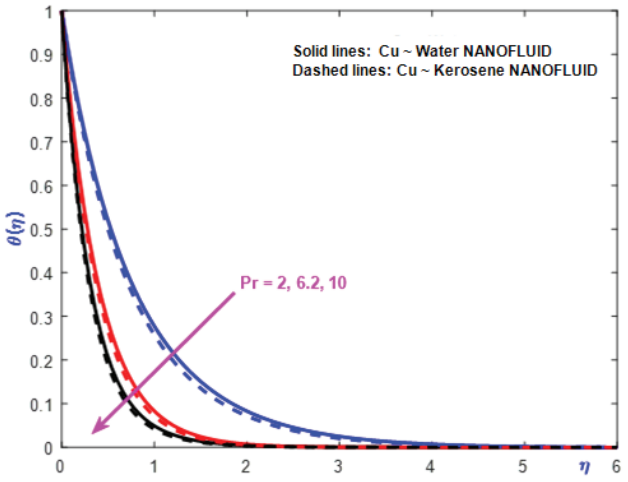

Figure 6. Influence of Prandtl number (Pr) on temperature.

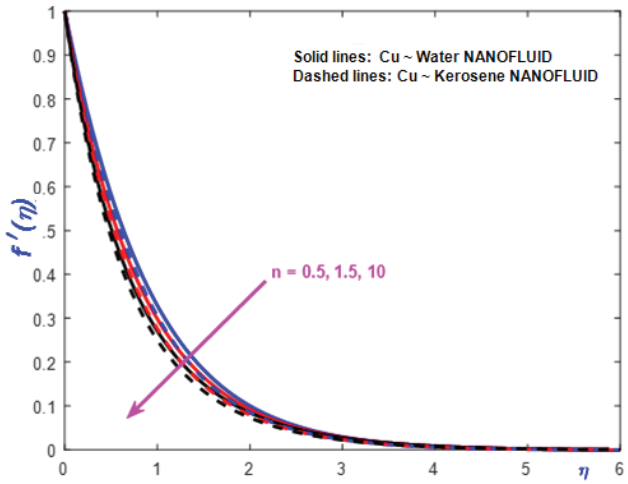

Figure 4. Influence of stretching parameter (n) on velocity.

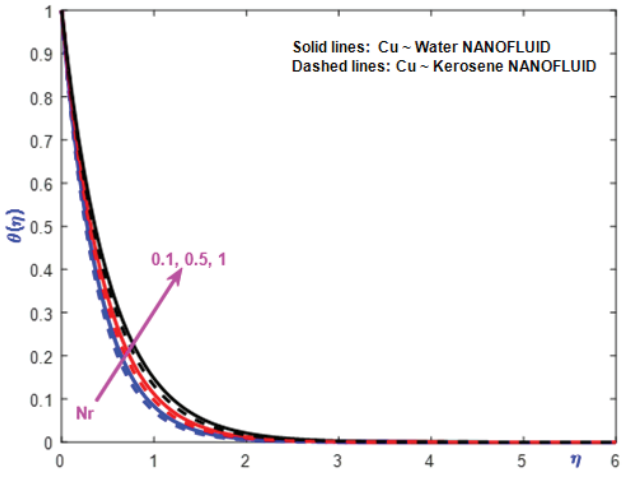

Figure 7. Influence of thermal radiation parameter (Nr) on temperature.

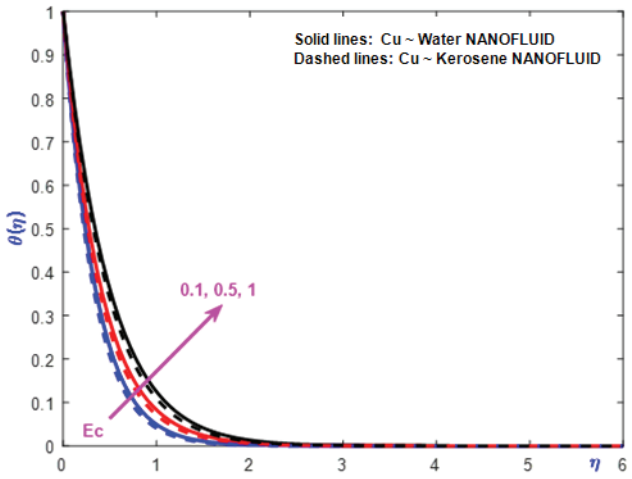

Figure 8. Influence of Eckert number (*Ec*)on temperature.

CONCLUSIONS

Simulated results for the flow of nanofluids in the presence of Cu nanoparticles over an expanding surface were carried out using water and kerosene-based liquids. On the other hand, the incorporation of thermal radiation and viscous dissipation encourages the occurrence of flow phenomena. The physical significance of the contributing parameters is depicted in graphs and tabular form to demonstrate their relationships. Furthermore, the following are the most significant observations made for both nanofluids:

- The comparative analysis in the particular case accumulated to the earlier study reveals a good correlation and also suggests the validation as well as the convergence criteria of the proposed methodology.
- The enhanced particle concentration, in conjunction with the nonlinear stretching parameter, retards the nanofluid velocity in either case of water and kerosene base fluids.
- The temperature profile becomes more pronounced for the enhanced radiation parameters, the solid volume fraction, and the Eckert number; however, the reverse trend is marked for the increasing Prandtl number and non-linear stretching parameter.
- Significant retardation in the shear rate coefficient is observed for the increasing particle concentration, whereas it overshoots the heat transfer rate.
- The combined effect of thermal radiation and the coupling parameter for the inclusion of dissipative heat, i.e. the augmented values of the Eckert number, decelerate the heat transfer rate.

Finally, but not least, Novelty of the current study not only illustrates the physical properties of the three defining parameters under specific conditions, but it also provides a roadmap for future research by incorporating the significant role of magnetic and electric fields in controlling fluid velocity, which will be beneficial for the manufacturing of a variety of products in the industrial sector, among other things. Using different particle sizes, on the other hand, will greatly assist in producing a finished product that is precisely the right form and size. Another reason to use an analytical method for the suggested governing equations is that it will be easier to compare them in the future.

NOMENCLATURE

C	constant
C_f	skin friction coefficient
C_p	specific heat capacity
Ec	Eckert number
k	thermal conductivity
n	nonlinear stretching parameter
Nu	Nusselt number
Nr	thermal radiation parameter
Pr	Prandtl number
T_∞	ambient temperature
$\tilde{T}_w$	wall temperature
$\overline{u}, \overline{v}$	velocity components along x and y directions
$\tilde{u}_w$	stretching velocity

Greek symbols

ρ	density
μ	viscosity
ϕ	solid volume fraction

Subscripts

f	base fluid
s	solid particle
nf	nanofluid

AUTHORSHIP CONTRIBUTIONS

Authors equally contributed to this work.

DATA AVAILABILITY STATEMENT

The authors confirm that the data that supports the findings of this study are available within the article. Raw data that support the finding of this study are available from the corresponding author, upon reasonable request.

CONFLICT OF INTEREST

The author declared no potential conflicts of interest with respect to the research, authorship, and/or publication of this article.

ETHICS

There are no ethical issues with the publication of this manuscript.

REFERENCES

[1] Choi SUS, Eastman JA. Enhancing thermal conductivity of fluids with nanoparticles. Conference: 1995 International mechanical engineering congress and exhibition, San Francisco, CA (United States), 12-17 Nov 1995 Other Information: PBD: Oct 1995, 1995;231:99−106. [CrossRef]

[2] Rashad AM, Abbasbandy S, Chamkha AJ. Non-Darcy natural convection from a vertical cylinder embedded in a thermally stratified and nanofluid-saturated porous media. J Heat Transf 2014;136:022503. [CrossRef]

[3] Ramreddy C, Murthy PVSN, Rashad AM, Chamkha AJ. Numerical study of thermally stratified nanofluid saturated non-Darcy porous medium. Eur Phys J Plus 2014;129:1−11. [CrossRef]

[4] El-Kabeir SMM, Chamkha AJ, Rashad AM. The effect of thermal radiation on non-darcy free convection from a vertical cylinder embedded in a nanofluid porous media. J Porous Media 2014;17:269−278. [CrossRef]

[5] Lin Y, Zheng L, Zhang X, Ma L, Chen G. MHD pseudo-plastic nanofluid unsteady flow and heat transfer in a finite thin film over stretching surface with internal heat generation. Int J Heat Mass Transf 2015;84:903−911. [CrossRef]

[6] Mishra SR, Pattnaik PK, Dash GC. Effect of heat source and double stratification on MHD free convection in a micropolar fluid. Alex Eng J 2015;54:681−689. [CrossRef]

[7] Bakar SA, Arifin NM, Nazar R, Ali FM, Pop I. Forced convection boundary layer stagnation-point flow in Darcy-Forchheimer porous medium past a shrinking sheet. Heat Mass Transf 2016;7:38. [CrossRef]

[8] Madhu M, Kishan N, Chamkha AJ. Unsteady flow of a Maxwell nanofluid over a stretching surface in the presence of magnetohydrodynamic and thermal radiation effects. Propuls Power Res 2017;6:31−40. [CrossRef]

[9] Mishra SR, Pattnaik PK, Bhatti MM, Abbas T. Analysis of heat and mass transfer with MHD and chemical reaction effects on viscoelastic fluid over a stretching sheet. Indian J Phys 2017;91:1219−1227. [CrossRef]

[10] Mustafa M. MHD nanofluid flow over a rotating disk with partial slip effects: Buongiorno model. Int J Heat Mass Transf 2017;108:1910−1916. [CrossRef]

[11] Qayyum S, Khan MI, Hayat T, Alsaedi A, Tamoor M. Entropy generation in dissipative flow of Williamson fluid between two rotating disks. Int J Heat Mass Transf 2018;127:933−942. [CrossRef]

[12] Afridi MI, Qasim M. Entropy generation and heat transfer in boundary layer flow over a thin needle moving in a parallel stream in the presence of non-linear Rosseland radiation. Int J Therm Sci 2018;123:117−128. [CrossRef]

[13] Khan MI, Hayat T, Khan MI, Alsaedi A. Activation energy Variations in non-linear radiative stagnation point flow of cross nanofluid. Int Commun Heat Mass Transf 2018;91:216−224. [CrossRef]

[14] Hayat T, Kiyani MZ, Alsaedi A, Khan MI, Ahmad I. Mixed convective three-dimensional flow of Williamson nanofluid subject to chemical reaction. Int J Heat Mass Transf 2018;127:422−429. [CrossRef]

[15] Jena S, Dash GC, Mishra SR. Chemical reaction effect on MHD viscoelastic fluid flow over a vertical stretching sheet with heat source/sink. Ain Shams Eng J 2018;9:1205−1213. [CrossRef]

[16] Mishra SR, Shahid A, Jena S, Bhatti MM. Buoyancy-driven chemicalized EMHD nanofluid flow through a stretching plate with Darcy-Brinkman-Forchheimer porous medium. Heat Transf Res 2019;50:1105−1126. [CrossRef]

[17] Mohapatra DK, Mishra SR, Jena S. Cu-Water and Cu-Kerosene micropolar nanofluid flow over a permeable stretching sheet. Heat Transf Asian Res 2019;48:2478−2496. [CrossRef]

[18] Sheikholeslami M, Sajjadi H, Delouei AA, Atashafrooz M, Li Z. Magnetic force and radiation influences on nanofluid transportation through a permeable media considering Al2O3 nanoparticles, mixed convection of a nanofluid in a three-dimensional channel. J Therm Anal Calorim 2019;136:2477−2485. [CrossRef]

[19] Pattnaik PK, Mishra SR, Barik AK, Mishra AK. Influence of chemical reaction on magnetohydrodynamic flow over an exponential stretching sheet: A numerical study. Int J Fluid Mech Res 2020;47:1−12. [CrossRef]

[20] Pattnaik PK, Mishra SR, Mahanthesh B, Gireesha BJ, Gorji MR. Heat transport of nano-Micropolar fluid with an exponential heat source on a convectively heated elongated plate using Numerical computation. Multidiscip Model Mater Struct 2020;16:1295−1312. [CrossRef]

[21] Pattnaik PK, Mishra SR, Bhatti MM. Duan-rach approach to study Al2O3-ethylene glycol C2H6O2 nanofluid flow based upon KKL model. Inventions 2021;5:45. [CrossRef]

[22] Jena S, Mishra SR, Pattnaik PK, Sharma RP. Nanofluid flow between parallel plates and heat transfer in presence of chemical reaction and porous matrix. Lat Am Appl Res 2020;50:283−289. [CrossRef]

[23] Acharya S, Nayak B, Mishra SR, Jena S. Adomian decomposition method for the MHD flow of a viscous fluid with the influence of dissipative heat energy. Heat Transf 2020;49:4612−4625. [CrossRef]

[24] Tshivhi KS, Makinde OD. Magneto-nanofluid coolants past heated shrinking/stretching surfaces: Dual solutions and stability analysis. Results Eng 2021;10:100229. [CrossRef]

[25] Ahmed MS, Elsaid AM. Effect of hybrid and single nanofluids on the performance characteristics of chilled water air conditioning system. Appl Therm Eng 2019;163:114398. [CrossRef]

[26] Elsaid AM. A novel approach for energy and mass transfer characteristics in wet cooling towers associated with vapor-compression air conditioning system by using MgO and TiO2 based H2O nanofluids. Energy Convers Manag 2020;204:112289. [CrossRef]

[27] Elsaid AM. Experimental study on the heat transfer performance and friction factor characteristics of Co_3O_4 and Al_2O_3 based $H_2O/(CH_2OH)_2$ nanofluids in a vehicle engine radiator. Int Commun Heat Mass Transf 2019;108:104263. [CrossRef]

[28] Elsaid AM, El-Said EM, Abdelaziz GB, Sharshir SW, El-Tahan HR, Abd Raboo MF. Performance and exergy analysis of different perforated rib designs of triple tubes heat exchanger employing hybrid nanofluids. Int J Therm Sci 2021;168:107006. [CrossRef]

[29] Mishra SR, Sun TC, Rout BC, Khan MI, Alaoui MK, Khan SU. Control of dusty nanofluid due to the interaction on dust particles in a conducting medium: Numerical investigation. Alex Eng J 2022;61:3341−3349. [CrossRef]

[30] Pattnaik PK, Mishra SR, Bég OA, Khan UF, Umavathi JC. Axisymmetric radiative titanium dioxide magnetic nanofluid flow on a stretching cylinder with homogeneous/heterogeneous reactions in Darcy-Forchheimer porous media: Intelligent nanocoating simulation. Mater Sci Eng B Solid State Mater Adv Technol 2022;277:115589. [CrossRef]

[31] Ramanuja M, Krishna GG, Nagaradhika V, Sreenadh S, Mishra SR. Channel flow of a Jeffrey fluid in a porous space with entropy generation. Heat Transf 2022; 51:2343−2361. [CrossRef]

[32] Hakeem AKA, Ragupathi P, Saranya S, Ganga B. Three dimensional non-linear radiative nanofluid flow over a riga plate. J Appl Comput Mech 2020;6:1012−1029.

[33] Ragupathi P, Hakeem AKA, Ganga B, Nadeem S. Three-dimensional viscous dissipative flow of nanofluids over a riga plate. J Heat Mass Transf Res 2021;8:49−60.

[34] Rashidi MM, Ganesh VN, Hakeem AKA, Ganga B. Buoyancy effect on MHD flow of nanofluid over a stretching sheet in the presence of thermal radiation. J Mol Liq 2014;198:234−238. [CrossRef]

[35] Ragupathi P, Hakeem AKA, Al-Mdallal Q, Ganga B, Shekar S. Non-uniform heat source/sink effects on the three-dimensional flow of Fe_3O_4/Al_2O_3 nanoparticles with different base fluids past a Riga plate. Case Stud Therm Eng 2019;15:100521. [CrossRef]

[36] Cortell R. Effects of viscous dissipation and radiation on the thermal boundary layer over a non-linearly stretching sheet. Phys Lett A 2008;372:631−636. [CrossRef]

[37] Brewster MQ. Thermal radiative transfer properties. 1st ed. New York: Wiley; 1992.

[38] Blasius H. Grenzschichtenin flüssigkeiten mit kleiner reibung. Zeitschrift für Angewandte Mathematik und Physik 1908;56:1−37. [Deutsch]

[39] Khan WA, Pop I. Boundary layer flow of a nanofluid past a stretching sheet. Int J Heat Mass Transf 2010;53:2477−2483. [CrossRef]

[40] Devi SSU, Devi SPA. Numerical investigation of three-dimensional hybrid Cu-Al_2O_3/water nanofluid flow over a stretching sheet with effecting Lorentz force subject to Newtonian heating. Can J Phys 2016;94:490−496. [CrossRef]